Eur. J. Biochem. 130, 497–508 (1983)

Sequential Individual Resonance Assignments in the ^1H Nuclear-Magnetic-Resonance Spectrum of Cardiotoxin $V^{II}2$ from *Naja mossambica mossambica*

Ramakrishna V. HOSUR, Gerhard WIDER, and Kurt WÜTHRICH

Institut für Molekularbiologie und Biophysik, Eidgenössische Technische Hochschule, Zürich

(Received September 10, 1982) – EJB 5988

The assignment of the ^1H nuclear magnetic resonance (NMR) spectrum of cardiotoxin $V^{II}2$ from *Naja mossambica mossambica* is described and documented. The assignments are based entirely on the amino acid sequence and on two-dimensional NMR experiments at 500 MHz. Individual assignments were obtained at 45 °C for the backbone protons of 56 out of the total of 60 amino acid residues, the exceptions being the N-terminal dipeptide segment Leu-1 – Lys-2 –, Pro-8 and Pro-15. Complete assignments of the non-labile hydrogen atoms of the side chains were obtained for 37 residues, and for Asn-4 and Asn-19 the δ amide protons were also identified. For 19 long side chains the individual assignments include only the backbone and C-β proton resonances; these are Gln-5, Pro-9, Pro-33, Pro-43, Leu-47, all three methionines, two arginines and nine lysines. The chemical shifts for the assigned resonances at 45 °C are listed for an aqueous solution at pH 3.6. A preliminary interpretation of the sequential connectivity patterns indicates that approximately 30 out of the total of 60 amino acid residues in cardiotoxin $V^{II}2$ are in extended, β-type secondary structures, and there is no indication for the formation of α-helical structure.

Polypeptide toxins from Elapidae venoms form a large family of homologous proteins. However, in spite of the sequence homologies, there are pronounced differences in the mode of action of different types of toxins [1, 2]. Thus, while neurotoxins bind to a protein receptor at the post-synaptic level and block acetylcholine reception [3], the action of membrane toxins results in a veriety of effects including hemolysis, cytotoxicity, depolarization of excitable membranes, and modulation of membranal enzyme activity [4, 5]. A common trait of the actions of the different membrane toxins at the cellular level appears to be binding to the cell membrane with disturbance of its organization and function [5 – 7]. Knowledge of the molecular conformation of any one membrane toxin might thus be informative with regard to this common feature of the functional properties of all proteins in this class. We have recently started investigations on the conformation of cardiotoxin $V^{II}2$ from *Naja mossambica mossambica* in aqueous solution and this is the second paper on nuclear magnetic resonance (NMR) experiments with this protein.

The preceding paper on this subject [8] reported on one-dimensional and two-dimensional NMR experiments with cardiotoxin $V^{II}2$ and a group of homologous toxin in ^2H_2O, which resulted in individual assignments of the resonance lines of five backbone amide protons, nine C-α protons, eleven C-β protons and the peripheral side-chain protons of all four aromatic amino acid residues and one isoleucine in the ^1H NMR spectrum of cardiotoxin $V^{II}2$ (see Table 1 for details). On the basis of these assignments and observation of nuclear Overhauser effects (NOEs) between the assigned protons, a triple-stranded β-sheet was proposed for a small region of the molecular structure of toxin $V^{II}2$.

Physical-chemical studies of snake toxin conformations (see [8] for a more comprehensive survey) include numerous NMR investigations of static and dynamic aspects of the three-dimensional protein structures [9 – 24]. Most of these NMR studies concentrated on neurotoxins and, to some degree, the interpretation of the NMR data relied on the known crystal structure of erabutoxin b [25 – 28]. In the present paper we make use of new procedures recently introduced [29 – 34] for obtaining nearly complete resonance assignments in the ^1H NMR spectrum of toxin $V^{II}2$. These assignments rely entirely on the amino acid sequence and on NMR data obtained by the use of two-dimensional NMR experiments in H_2O solution of the protein at 500 MHz.

MATERIALS AND METHODS

Cardiotoxin $V^{II}2$ from *Naja mossambica mossambica* was obtained as a gift from Prof. M. Lazdunski of the University of Nice. The isolation procedure was described previously [35]. About 17 mg of the protein was lyophilised and dissolved in a volume of about 0.3 ml to obtain roughly 0.01 M solutions in the following solvents: (a) 90 % H_2O + 10 % ^2H_2O, pH 3.6; (b) ^2H_2O, p^{2}H 3.6. In the latter sample the labile amide protons were fully exchanged with ^2H by heating the ^2H_2O solution to 50 °C for 2 h, and the residual water protons were minimised by repeated lyophilisation.

The two-dimensional NMR experiments used were previously described in detail (e. g. [29, 30, 33, 34, 36 – 41]) and are therefore only briefly outlined here. ^1H-^1H *J*-connectivity maps were obtained with two-dimensional correlated spectroscopy (COSY) and spin-echo correlated spectroscopy (SECSY). COSY uses the pulse sequence [36 – 38] $(90° - t_1 - 90° - t_2)_n$, where t_1 and t_2 are the evolution period and the observation period, respectively. To obtain a 2D NMR spectrum, the

Abbreviations. δ, chemical shift; 2D NMR, two-dimensional nuclear magnetic resonance, NOE, nuclear Overhauser effect; ppm, parts per million; SECSY, two-dimensional spin-echo correlated spectroscopy; toxin $V^{II}2$, cardiotoxin $V^{II}2$ from *Naja mossambica mossambica*; NOESY, two-dimensional nuclear Overhauser enhancement spectroscopy; COSY, two-dimensional correlated spectroscopy; in the figures, amino acids are abbreviated by the one-letter system, see *Eur. J. Biochem.* 5, 151 – 153 (1968).

measurement is repeated for a set of equidistant t_1 values. To improve the signal-to-noise ratio, n transients are accumulated for each value of t_1. At the end of each transient, the system was allowed to reach equilibrium during a fixed delay of 1 s. All the COSY spectra reported here were obtained either from 350 or from 400 measurements, using t_1 values from 0.3 ms to 35 ms, or from 0.3 ms to 40 ms, respectively. The aquisition time in the ω_2 direction was 100 ms.

SECSY uses the pulse sequence [37, 39] $(90^\circ - t/_1/2 - 90^\circ - t_1/2 - t_2)_n$. The SECSY spectrum of Fig. 1 was obtained from 400 measurements corresponding to t_1 values from 0.3 ms to 214 ms.

^{1}H-^{1}H NOE connectivity maps were obtained with 2D nuclear Overhauser enhancement spectroscopy (NOESY), using the pulse sequence [40, 41] $(90^\circ - t_1 - 90^\circ - \tau_m - 90^\circ - t_2)_n$, where τ_m is the so-called mixing time. The NOESY spectra used were obtained from 350 or 400 measurements, corresponding to t_1 values from 0.3 ms to 35 ms or to 40 ms, respectively. The mixing time was 100 ms. In order to suppress contributions from coherent magnetisation transfer to the cross peak intensities, the mixing time was stochastically modulated with a modulation amplitude of 5% of the mixing time [42].

The 2D NMR spectra were recorded at 500 MHz on a Bruker WM 500 spectrometer. Quadrature detection was used, with the carrier frequency placed at the low-field end of the spectrum. The free induction decays for COSY and NOESY were collected with 2048 points in the t_2 direction, while SECSY used 3800 points. To eliminate experimental artifacts, groups of 16 recordings with different phases for the 90° pulses were added for each value of t_1 [37, 39]. For measurements in H_2O, the solvent resonance was suppressed by selective continuous irradiation at all times except during data collection [43, 44]. For COSY and NOESY the time domain data matrix was expanded by 'zero filling' to 2048 points in t_1 and to 4096 points in t_2 and then Fourier-transformed to end up with a 1024 × 1024 point frequency domain data matrix. This resulted in a digital resolution of 4.9 Hz/point for the spectra recorded in H_2O and of 3.6 Hz/point for the spectra recorded in ^2H_2O. For the SECSY spectrum, the time domain data matrix was expanded to 1024 points in t_1 and to 8192 points in t_2. After Fourier transformation this resulted in a digital resolution of 1.8 Hz/point in both the ω_1 and ω_2 directions. Before Fourier transformation the time domain data matrix was multiplied in all spectra with a phase-shifted sine bell, $\sin[\pi(t+t_o)/t_s]$, in the t_1 direction and with a phase-shifted sine-squared bell, $\sin^2[\pi(t+t_o)/t_s]$, in the t_2 direction. The length of the window functions, t_s, was adjusted for the bells to reach zero at the last experimental point in the t_1 and t_2 directions. The phase shifts, t_o/t_s, were 1/64 and 1/128 in the t_1 and t_2 direction, respectively. In some plots of COSY and NOESY only the first 1024 experimental points were used in the t_2 direction so as to enhance the signal-to-noise ratio. All the spectra are shown in the absolute value representation.

RESULTS

In earlier experiments [8] 360-MHz ^{1}H NMR spectra of toxin V^{II}2 in ^2H_2O solution were analyzed and a limited number of resonance lines could be assigned (see Table 1). The previous observation that these spectra contain numerous well defined peaks is confirmed by the 500-MHz ^{1}H SECSY spectra of Fig. 1 and 2, which were also recorded in ^2H_2O solution. The spectral analysis in the present paper, however, relies largely on spectra recorded in H_2O solution. As an illustration, Fig. 3 shows a 500-MHz NOESY spectrum of toxin V^{II}2. It can be

Table 1. *Chemical shifts, δ, of assigned resonances in the ^{1}H NMR spectrum of cardiotoxin V^{II}2 from* Naja mossambica mossambica *at pH 3.6, 45 °C*

Chemical shifts are expressed relative to the internal standard sodium 3-trimethylsilyl-(2,2,3,3-$^2H_4$)propionate. They are accurate to ±0.02 ppm. The residues have been numbered consecutively. Proper deletions should be inserted in the sequence for comparison with homologous toxins [4, 8]. Where no numbers are given in the columns for NH, C$^\alpha$H C$^\beta$H, and where more peripheral side chain atoms are not listed in the last column, no individual resonance assignments were obtained (see text). When the resonance assignments listed in this table were completed, three resolved methyl doublets in the ^{1}H NMR spectrum at 0.60 ppm, 0.99 ppm and 1.03 ppm remained unassigned. While it is clear that these lines must correspond to methyl groups in Leu-1, Leu-47 and possibly Leu-20 (see text), they could not be individually connected to particular ones of these residues

Amino acid residue	Chemical shift, δ, for protons			
	amide	C-α	C-β	others
	ppm			
Leu-1				
Lys-2				
Cys-3	9.25	5.21	2.67, 2.78	
Asn-4	9.59	5.44	2.19, 2.66	N$^\delta$H$_2$ 7.83
Gln-5	7.91	4.84	2.50, 2.79	
Leu-6	8.28	4.11	1.44, 1.60	C$^\gamma$H 1.71 C$^\delta$H$_3$ 0.84, 0.95
Ile-7	7.79	4.19	1.53	C$^\gamma$H$_3$ 0.75 C$^\gamma$H$_2$ 1.48, 1.64 C$^\delta$H$_3$ 0.83
Pro-8				
Pro-9		4.73	1.76, 1.90	
Phe-10[a]	8.78	4.11	3.70	C-2, 6 H$_2$ 7.36 C-3, 5 H$_2$ 7.12 C-4 H 7.21
Trp-11[a]	8.61	5.57	3.00, 3.48	C-2 H 7.30 C-4H 7.36 C-5 H 7.12 C-6 H 7.21 C-7 H 7.50
Lys-12	8.80	5.21	1.96, 2.18	
Thr-13	8.66	4.79	4.06	C$^\gamma$H$_3$ 1.29
Cys-14	9.09	4.97	2.77, 3.48	
Pro-15				
Lys-16	7.53	3.99	1.67, 1.67	
Gly-17	8.72	4.27 3.66		
Lys-18	7.58	4.29	1.61, 1.83	
Asn-19	7.88	4.90	2.21, 2.46	N$^\delta$H$_2$ 8.66
Leu-20[a]	8.11	4.79[a]	2.05, 2.05	C$^\gamma$H 1.84 C$^\delta$H$_3$ 0.95
Cys-21[a]	8.96	6.06	2.98, 3.07	
Tyr-22[a]	9.18	6.20	3.04, 3.19	C-2, 6H 6.76 C-3, 5H 6.68
Lys-23	9.25[a]	4.79[a]	1.33, 1.63	
Met-24[b]	8.56	5.27	1.69, 1.91	
Thr-25	9.02	4.68	4.07	C$^\gamma$H$_3$ 1.04
Met-26[b]	8.75	5.06	1.85, 2.12	
Arg-27	8.40	4.09	1.80, 1.81	
Gly-28	8.56	3.84 4.13		
Ala-29	7.98	4.63	1.33	
Ser-30	7.52	4.94	3.94, 4.39	
Lys-31	9.59	3.49	2.22	
Val-32	8.97	4.35	1.52	C$^\gamma$H$_3$ 0.69, 0.71
Pro-33		4.00	1.34, 1.81	
Val-34	7.61	4.01	1.70	C$^\gamma$H$_3$ 0.70, 0.74

Table 1 (continued)

Amino acid residue	Chemical shift, δ, for protons			
	amide	C-α	C-β	others
	ppm			
Lys-35	8.28	4.03	1.66, 1.80	
Arg-36	7.99	4.24	1.79	
Gly-37	8.46	4.13		
		4.33		
Cys-38	8.85	5.94[a]	2.91[a], 3.55[a]	
Ile-39[a]	9.74	4.37	1.66	$C^{\gamma}H_2$ 1.35, 1.56
				$C^{\gamma}H_3$ 0.49
				$C^{\delta}H_3$ 0.31
Asp-40	8.56	5.16	2.45, 3.00	
Val-41	7.47	4.35	2.06	$C^{\gamma}H_3$ 0.88, 0.89
Cys-42	8.37	4.33	2.21, 2.71	
Pro-43		4.25	1.65	
Lys-44	8.70	4.51	1.77, 2.05	
Ser-45	8.67	4.84	4.04, 4.43	
Ser-46	9.06	4.26	3.85, 3.92	
Leu-47	8.11	4.29	1.74, 1.95	
Leu-48	8.32	4.23	1.36, 1.72	$C^{\gamma}H$ 1.43
				$C^{\delta}H_3$ 0.83, 1.02
Ile-49	7.86	4.43	1.66	$C^{\gamma}H_2$ 1.04, 1.31
				$C^{\gamma}H_3$ 0.89
				$C^{\delta}H_3$ 0.81
Lys-50	9.43	4.91	1.76	
Tyr-51	7.26	4.51	2.71, 3.02	C-2, 6H[a] 6.83
				C-3, 5H[a] 6.71
Met-52[b]	7.45	5.54	1.86, 2.05	
Cys-53	9.07	5.82[a]	2.99[a], 3.76[a]	
Cys-54	9.15[a]	5.08[a]	2.62, 3.33	
Asn-55	8.55	4.90	2.62, 2.99	
Thr-56	7.50	4.66	4.23	$C^{\gamma}H_3$ 1.17
Asp-57	7.42	5.06	3.42, 3.59	
Lys-58	8.45	4.84		
Cys-59	9.43	5.00	2.56, 2.71	
Asn-60	8.28	4.44	3.33, 3.59	

[a] Amino acids or individual resonances which were previously assigned [8]. Small differences between the chemical shifts in the present and the previous publication [8] must be attributed to the improved resolution at 500 MHz.

[b] The three Met εCH_3 singlets were already identified in earlier experiments [8] but could not be individually assigned. The line at 1.97 ppm was tentatively assigned to Met-24.

seen that this spectrum contains a large number of well defined and quite intense cross peaks, which indicates that the protein adopts a well defined conformation with restricted mobility for the bulk of the polypeptide backbone and many of the amino acid side chains. In the COSY spectra recorded in H_2O solution of toxin $V^{II}2$, the number of cross peaks between amide protons and C-α protons coincided closely with the 'NMR fingerprint' [33] expected from the amino acid sequence [4] (see Fig. 11 below), indicating that the resonances of all, or nearly all, the amino acid residues can be resolved in the 2D NMR spectra of this protein. In the following, individual assignments of the resonances in these spectra are described and documented for all those residues for which this data was not previously obtained [8].

Identification of Complete Amino-Acid Side-Chain Spin Systems before Sequential Assignments of the Polypeptide Backbone Protons

Here, the spin systems of different types of amino acid residues are identified. From this first step of the spectral analysis, assignments to specific positions in the amino acid sequence are obtained only when there are single residues with unique spin systems [29], such as Ala-29 in toxin $V^{II}2$. Toxin $V^{II}2$ contains 3 Gly, 1 Ala, 3 Val, 5 Leu, 3 Ile, 5 Pro, 3 Ser, 3 Thr, 2 Asp, 4 Asn, 1 Gln, 10 Lys, 2 Arg, 8 Cys, 3 Met, 1 Phe, 2 Tyr and 1 Trp. The SECSY spectrum of the protein was screened for the cross peak patterns which are characteristic for the different types of amino acid residues [29]. The resulting spin system identifications in toxin $V^{II}2$ are documented in Fig. 1 and 2. It is seen that in this first step the complete spin systems were identified for all three glycines, all three threonines, all three valines, the single alanine, one isoleucine and, combined with the previous identifications of the $C^{\alpha}H$-$C^{\beta}H_2$ fragments of Trp-11, Cys-21, Tyr-22, Cys-28 and Cys-54 [8], all 21 $C^{\alpha}H$-$C^{\beta}H_2$ three-spin systems. The individual assignments, which resulted from the additional studies described below, are also indicated in Fig. 1 and 2.

Sequential Resonance Assignments for the Polypeptide Backbone Protons

Here we follow a strategy which relies on stereochemical considerations [32, 46] of polypeptides and the use of 2D NMR experiments in H_2O solution of the protein [30, 33, 34]. Two crucial steps may be distinguished. Firstly, neighbouring residues in the amino acid sequence are identified. Since hydrogen atoms in sequentially adjoining amino acid residues are separated by four or more covalent bonds (Fig. 4), the spin-spin coupling constants are too small to be used for this purpose. Therefore, the crucial quantities for the identification of neighbouring residues are the distances d_1, d_2 and d_3 between the amide proton of residue $i+1$ and the C-α proton, the amide proton and the C-β protons, respectively, of the preceding residue i (Fig. 4). Since each of the three distances d_1, d_2 and d_3 depends on at least one of the torsion angles ϕ_i, ψ_i and χ_i^1, different connectivities are to be expected for different segments of the polypeptide chain, depending on the secondary structure [32, 46–48]. The intrinsic reliability of the identification of sequentially neighburing amino acid residues is of the order of 80% when it is based on the observation of one of these through-space connectivities, and of the order of 90% when it is based on any two of the three connectivities [32]. These values for the reliability that d_1, d_2 and d_3 provide connectivities between neighbouring residues were obtained with the assumption that only proton-proton distances ≤ 0.3 nm are manifested in the NOESY spectra used for resonance assignments, and from a statistical evaluation of the relative frequencies with which short d_1-type, d_2-type and d_3-type distances occur between neighbouring and non-neighbouring amino acids in refined crystal structures of globular proteins [32].

The identification of neighbouring residues typically results in connectivities which extend over peptide segments of from two to about six residues. The second crucial step then consists in locating these segments in the amino acid sequence. For this the data on the identification of amino-acid side-chain spin systems (Fig. 1 and 2 [8]) are combined with the sequential assignments obtained from d_1, d_2 and d_3 (Fig. 4). The two data sets overlap for the $C^{\alpha}H$-$C^{\beta}H_n$ fragments of the individual residues. On this basis the residues in the connected peptide

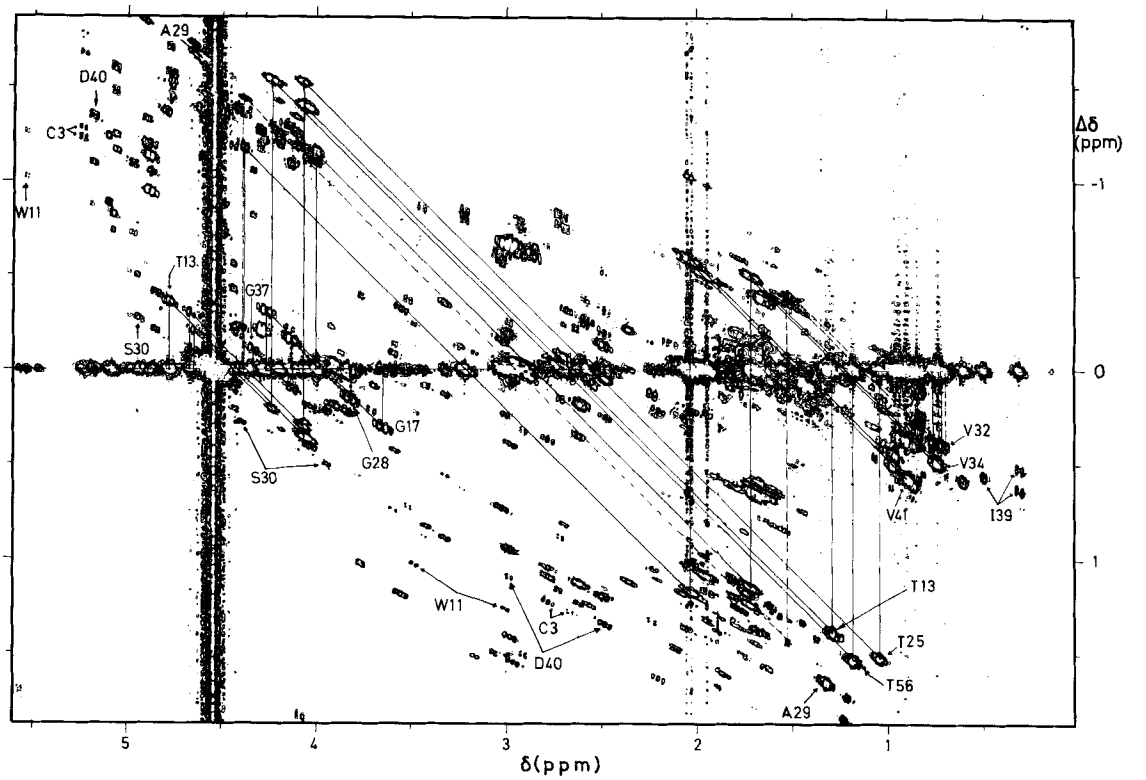

Fig. 1. *Contour plot of the region from 0 to 5.6 ppm of a 500-MHz ^1H SECSY spectrum of a 0.01 M solution of toxin $V^{II}2$ in ^2H_2O; p^2H 3.6, 45 °C.* The spectrum was recorded in about 46 h. Proton-proton *J* connectivities are shown for the following amino acid side chains: Val-32 (-----), Val-34 (———), Val-41 (———), Thr-13 (— —), Thr-25 (– ——), Thr-56 (— — —), Gly-17 (–——), Gly-28 (·····) and Gly-37 (———). In order not to overcrowd the figure a simplified representation is used for the AMX spin systems of Ser-30, Asp-40, Cys-3 and Trp-11, whereby the $C^{\alpha}H$-$C^{\beta}H_2$ cross peaks are identified by arrows but not connected by lines, and the $C^{\beta}H$-$C^{\beta'}H$ cross peaks are not identified. The cross peaks for Ala-29 and those involving the previously identified methyl groups of Ile-39 are also indicated

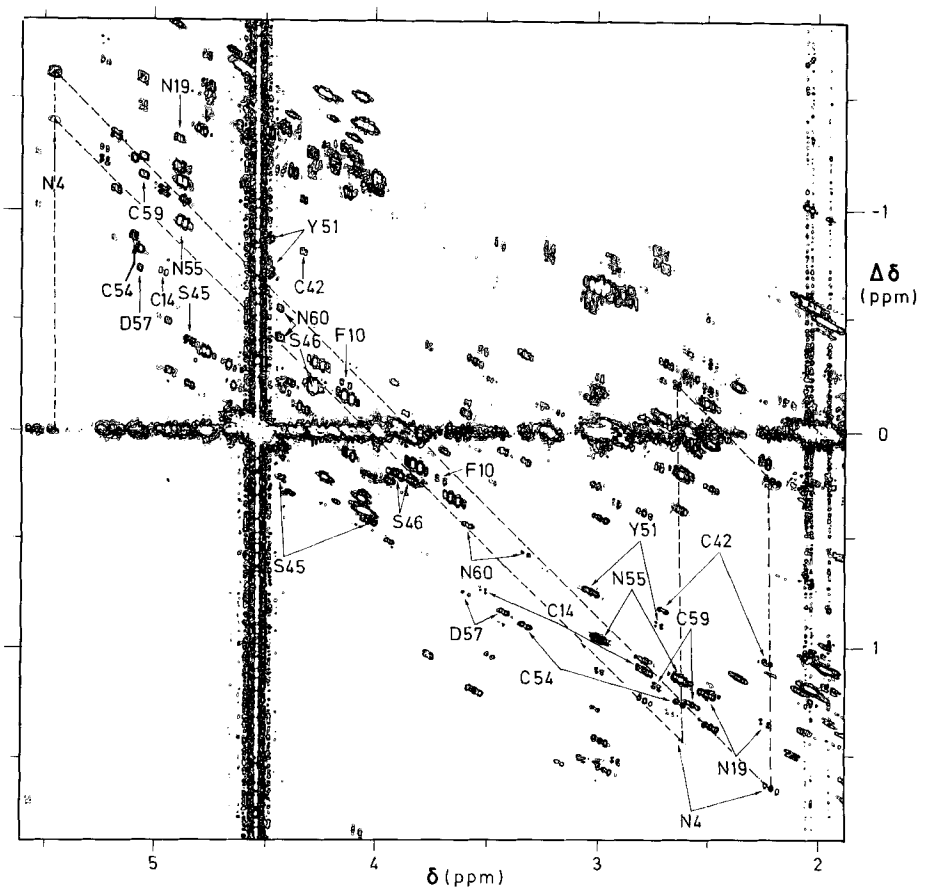

Fig. 2

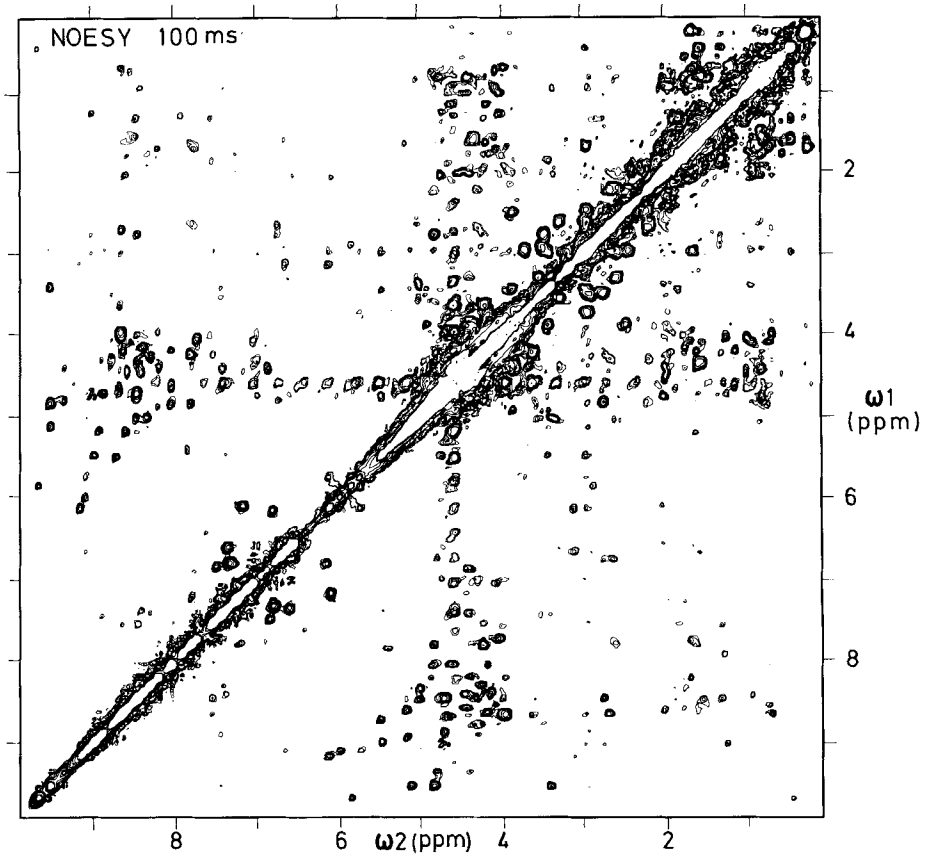

Fig. 3. *Contour plot of a symmetrical [45] absolute-value ^1H NOESY spectrum of toxin $V^{II}2$ at 500 MHz.* The spectrum was recorded in a 0.01 M solution of the protein in a mixed solvent of 90% H_2O and 10% ^2H_2O, pH 3.6 at 45 °C. The mixing time was 100 ms. The spectrum was recorded in about 83 h

segments can be assigned to unique amino acid types or to a group of amino acids (e.g. 'AMX spin systems' or 'long side chains') and subsequently these segments can be matched against corresponding sequences of residues in the primary structure. Obviously, this is most straightforward when the segment in question contains a residue type which occurs only once in the protein, e.g. Ala-29 in toxin $V^{II}2$ (Fig. 5). Once the location in the amino acid sequence has thus been established, further sequential assignments can be checked against the sequence. For example, when starting from Ala-29 in toxin $V^{II}2$, sequential assignments in the direction towards the N terminus must lead to Gly-28 – Arg-27 (≡ 'long side chain') – Met-26(≡ 'long side chain') – Thr-25-, and in the direction towards the C terminus to Ser-30 (≡ AMX) – Lys-31 (≡ 'long side chain') – Val-32-. Obviously the reliability of each step in the sequential assignments is further increased when the spectral analysis has reached this stage.

Fig. 5 presents a survey of the sequential assignments obtained for toxin $V^{II}2$. The chemical shifts for the assigned resonances are listed in Table 1. It is seen that for almost the entire sequence sequential assignments of the backbone protons were obtained and that many of the connectivities are based on observation of either d_1 and d_3, or d_2 and d_3. The sequential connectivities are documented in Fig. 6 – 10, whereby at least one connectivity is shown for each pair of neighbouring residues.

In Fig. 6 – 8 d_1 connectivities in toxin $V^{II}2$ are documented in combined COSY/NOESY connectivity diagrams [30]. These diagrams make use of the fact that the information in a COSY or NOESY spectrum is contained redundantly in the two triangles separated by the diagonal peaks (Fig. 3). When the upper-left triangle of NOESY and the lower-right triangle of COSY are added[1], the combined plot manifests through-space NOE connectivities as well as through-bond J connectivities. In contrast to the previous connectivity diagrams which used the entire spectrum [30], only those spectral regions are displayed in Fig. 6 – 8 which contain the connectivities between amide and C-α protons, and the diagonal peaks are substituted by a virtual diagonal. In these plots a record of sequential assignments via d_1 in the direction towards the N terminus consists of a counterclockwise, spiral-like connectivity pattern. This is most readily illustrated by a description of the assignments for one of the peptide segments in Fig. 6 – 8,

[1] In practice the spectra were used without being made symmetrical [45], and to evade interference with the strong vertical tail of the water resonance (see e. g. [30, 33, 43]), the mirror image of the upper-left triangle of the COSY spectrum was used.

Fig. 2. *Contour plot of the spectral region from 2.0 ppm to 5.5 ppm of the same SECSY spectrum of toxin $V^{II}2$ as in Fig. 1.* The complete connectivity pattern for the J cross peaks of AMX spin systems is illustrated for Asn-4 (- - - - -). For the AMX spin systems of Cys-54, Cys-59, Asp-57, Asn-19, Cys-14, Asn-55, Ser-45, Cys-42 and Phe-10, the $C^{\alpha}H$ chemical shifts are indicated by vertical arrows and the $C^{\beta}H_2$-$C^{\alpha}H$ cross peaks are individually identified. For Tyr-51, Asn-60 and Ser-46, the cross peaks at the $C^{\alpha}H$ and $C^{\beta}H_2$ chemical shifts are identified by arrows

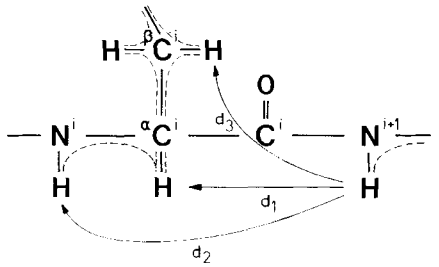

Fig. 4. *Polypeptide backbone segment.* The through-space distances d_1, d_2 and d_3 between hydrogen atoms located in neighbouring residues are indicated by arrows. The broken lines indicate through-bond J connectivities between different hydrogen atoms within the residues i and $i+1$

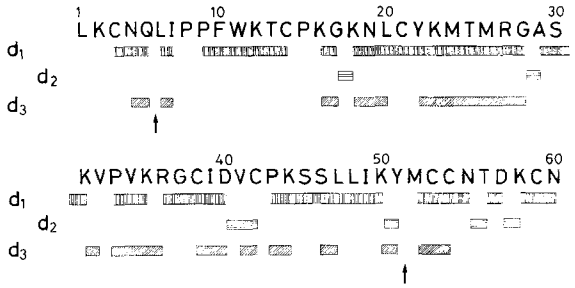

Fig. 5. *Amino acid sequence of cardiotoxin V[II]2 from* Naja mossambica mossambica. Note that the residues have been numbered consecutively, in contrast to the preceding paper [8], where the homology assignment of Karlsson [4] was used; proper deletions must therefore be accounted for when comparisons with the earlier data are made. The figure also shows the sequential connectivities by which the individual resonance assignments listed in Table 1 were obtained. Vertically shaded blocks indicate sequential assignments via d_1 (NOE from NH_{i+1} to $C^{\alpha}H_i$); horizontally shaded blocks indicate sequential assignments via d_2 (NOE from NH_{i+1} to NH_i); diagonally shaded blocks indicate sequential assignments via d_3 (NOE from NH_{i+1} to $C^{\beta}H_i$). The arrows indicate locations where the connectivity between two adjoining residues could not be established even through all the protons had been assigned

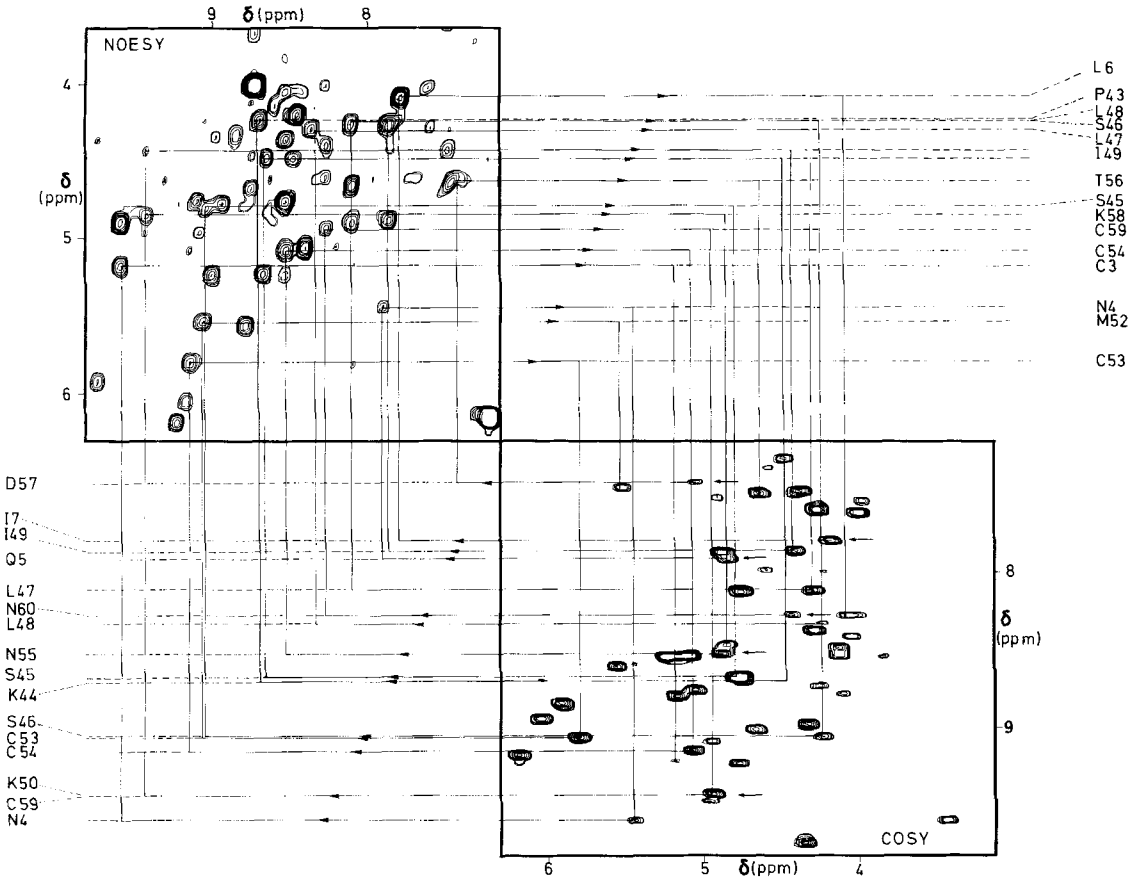

Fig. 6. *Combined COSY/NOESY connectivity diagram for sequential resonance assignments via NOEs between amide protons and the C-α protons of the preceding residue* (d_1). In the upper-left corner the region (ω_1 = 3.7–6.4 ppm, ω_2 = 7.2–9.8 ppm) of the ^{1}H NOESY spectrum of cardiotoxin V[II]2 in Fig. 3 is presented. In the lower-right corner the region (ω_1 = 7.2–9.8 ppm, ω_2 = 3.2–6.4 ppm) from a ^{1}H COSY spectrum recorded from the same sample under identical conditions, i. e. 45 °C and pH 3.6, is shown. The straight lines and arrows indicate the connectivities between neighbouring residues in the segments 5–3, 7–6, 50–43, 55–52, 57–56 and 60–58. Arrows identify the start for each segment. The amide proton chemical shifts are indicated by the assignments in the lower-left corner, those for the C-α protons by the assignments in the upper-right corner of the figure. In this spectrum the COSY cross peak of Lys-44 was bleached out by the irradiation of the water resonance [43, 44], but it was observed in different experiments (see Fig. 11)

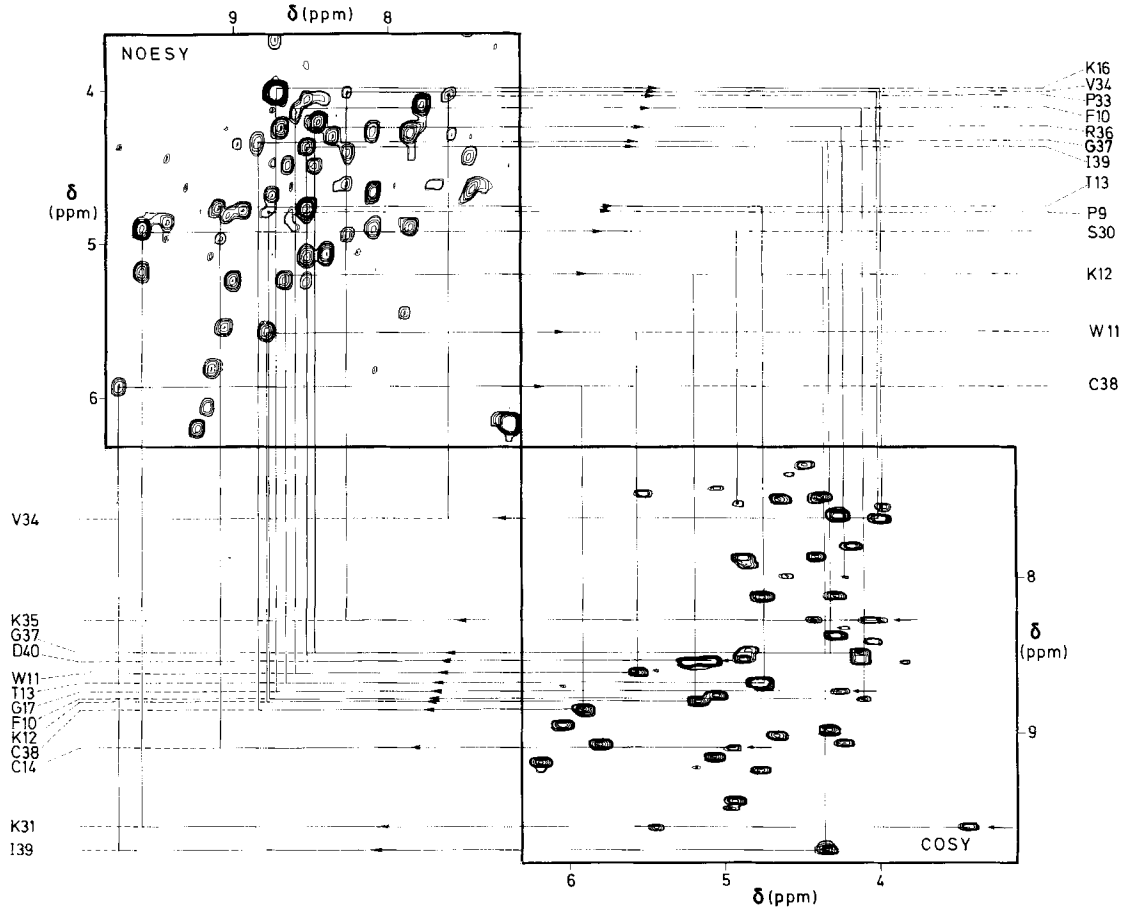

Fig. 7. *Combined COSY/NOESY* d_1 *connectivity diagram with the same spectra and same presentation as in Fig. 6.* The connectivity patterns are indicated with solid lines for the following segments of the toxin $V^{II}2$ polypeptide chain: 14 – 9, 17 – 16, 31 – 30, 35 – 33 and 40 – 36. Note that Gly-37 represents a special situation. One C-α proton yields a strong d_1 connectivity with Cys-38 in NOESY, but gives only a weak COSY cross peak with the amide proton (Fig. 11), which is absent in the plot used here. The second C-α proton gives a strong COSY peak but does not manifest a d_1 connectivity

say for Gln-5 to Cys-3. From the $C^{\alpha}H$-NH cross peak of Gln-5 in the COSY part of Fig. 6, a horizontal line leads to the virtual diagonal position of the amide proton resonance of Gln-5. There is a single NOESY cross peak with the Gln-5 NH chemical shift, which is therefore assigned to $C^{\alpha}H$ of Asn-4. In Fig. 6 a vertical line connects this peak with the diagonal position of Gln-5 NH. Continuing on, a horizontal line leads to the virtual diagonal position of $C^{\alpha}H$ of Asn-4. From there a vertical line connects with the $C^{\alpha}H$-NH COSY peak of Asn-4, which is then connected in NOESY with Cys-3. The connectivity patterns ends at the NH-$C^{\alpha}H$ COSY cross peak of Cys-3. Consultation of Fig. 4 shows that the connectivity patterns in the combined COSY/NOESY diagrams correspond to a step-by-step walk along the polypeptide chain, whereby a d_1 connectctivity in NOESY is always followed by a J connectivity in COSY, and vice versa. From Fig. 4 it is further readily apparent that the d_1 connectivity patterns for the segments 50 – 43 (Fig. 6), 35 – 33 and 14 – 9 (Fig. 7) must end with the NOESY cross peak to $C^{\alpha}H$ of proline, since proline does not contain an amide proton.

In Fig. 9 d_2 connectivities (Fig. 4) in toxin $V^{II}2$ are documented in the NOESY spectrum. In this presentation [33] the diagonal amide proton resonances of neighbouring residues are connected via the NOE cross peaks. Since in contrast to d_1 and d_3, d_2 is symmetrical with respect to the direction of the polypeptide chain (Fig. 4), d_2 connectivities from a given residue to the amide protons of both the preceding and the following residue in the sequence may be seen [32, 33].

The sequential connectivities between residues Lys-31 and Val-32, and between Lys-35 and Arg-36 were established via d_3 (Fig. 5). These two d_3 connectivities are documented in Fig. 10.

A further check of the sequential resonance assignments surveyed in Fig. 5 and documented in Fig. 6 – 10 is provided by the NH_i-$C^{\alpha}H_i$ region of the COSY spectrum of toxin $V^{II}2$ in H_2O (Fig. 11). In this spectral region each residue gives rise to one peak, with the exception of glycine, which may give one or two peaks, proline, which is not represented in this region, and possibly the residues in the N-terminal dipeptide segment, where the NH exchange with the solvent may be too fast for the cross peaks to be observed. In Fig. 11, all the strong cross peaks and some weaker peaks have been assigned to particular amino acid residues, and each peak has been assigned only once. The NH-$C^{\alpha}H$ region contains a number of additional, mostly weak cross peaks, which have as yet not been assigned. Possible origins of these additional peaks will be discussed below.

Further Individual Resonance Assignments of Amino-Acid Side-Chain Protons after Sequential Assignments fo the Polypeptide Backbone

Once any one of the three connectivities d_1, d_2 or d_3 is established, assignments for additional protons within the same

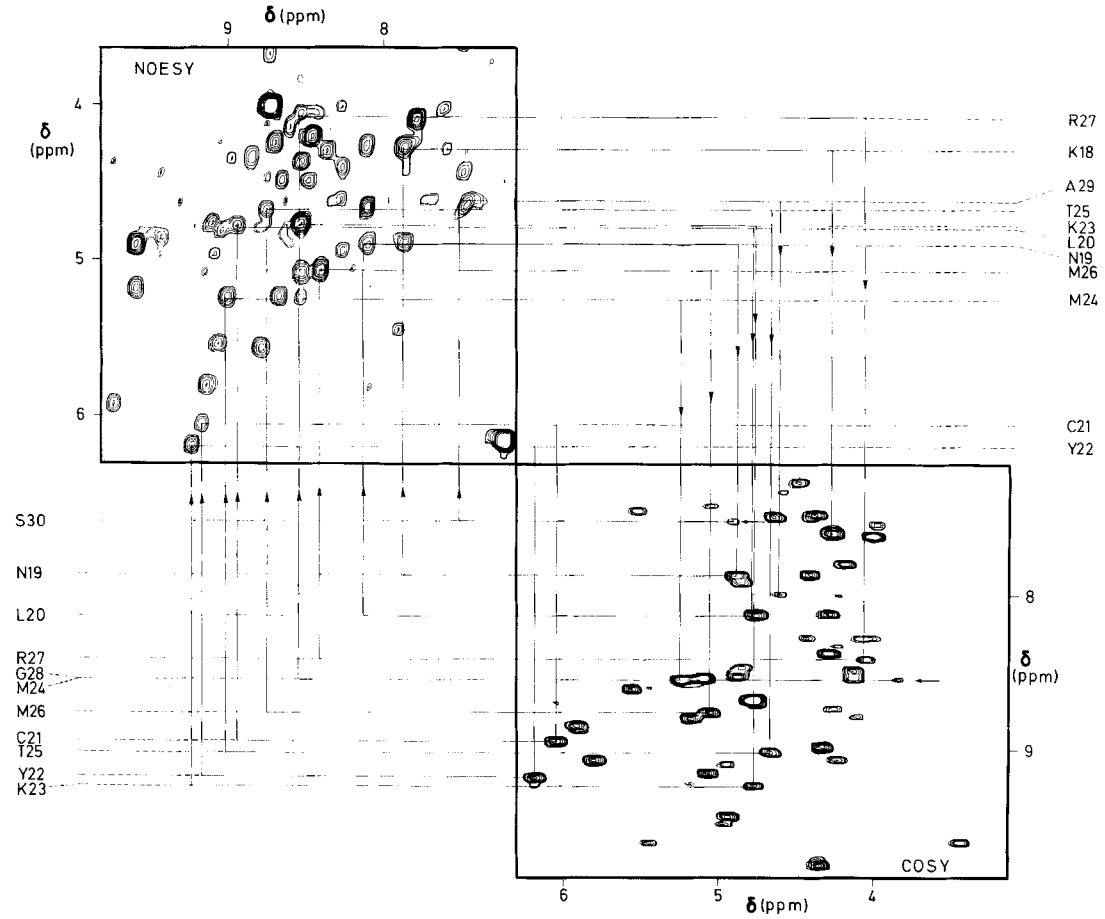

Fig. 8. *Combined COSY/NOESY* d_1 *connectivity diagram with the same spectra and same presentation as in Fig. 6.* The connectivity patterns are indicated with solid lines for the following segments of the toxin $V^{II}2$ polypeptide chain: 30–29 and 28–18

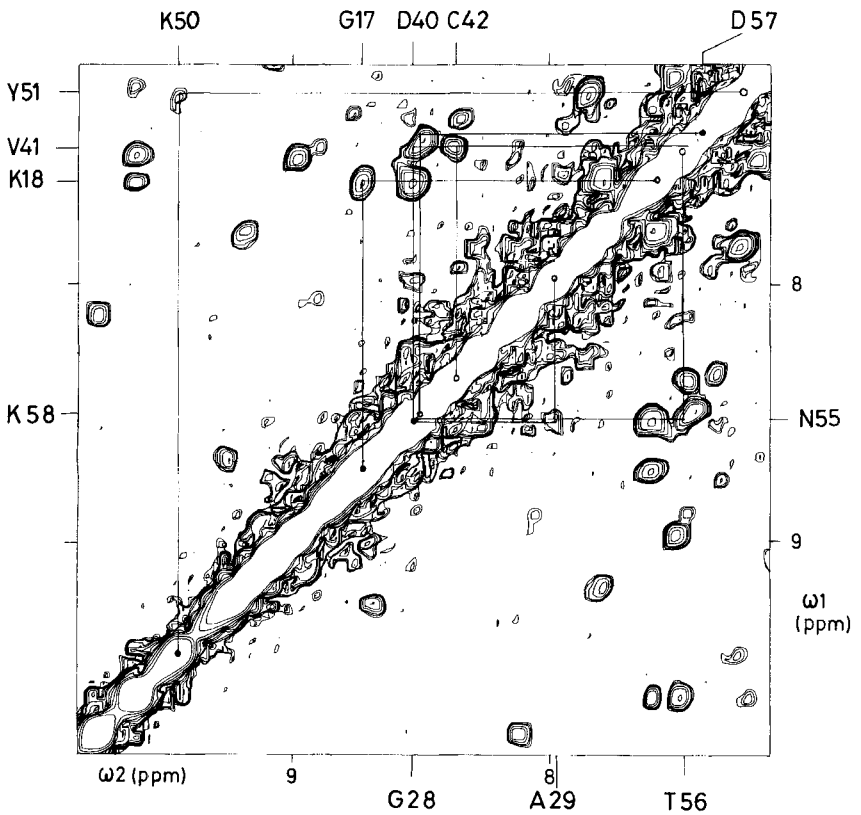

Fig. 9. *Contour plot of the spectral region from 7.2 ppm to 9.8 ppm of the 500-MHz* ^1H *NOESY spectrum of Fig. 3.* The spectrum was recorded from a solution of toxin $V^{II}2$ in H_2O at pH 3.6 and 45 C, with a mixing time of 100 ms. This spectral region contains the diagonal peaks of the bulk of the backbone amide protons and many cross peaks which manifest NOEs between different amide protons. d_2 connectivities between neighbouring residues are indicated by the solid lines, and the resonance positions and assignment of the connected amide protons are indicated in the margins of the figure. The upper-left triangle contains the connectivities for the polypeptide segments 50–51, 17–18, 40–42 and 57–58. The lower right triangle contains the connectivities for the segments 28–29 and 55–56. Filled circles (●) and open circles (○), respectively, indicate the start and the end of the d_2 connectivity patterns for the individual peptide segments

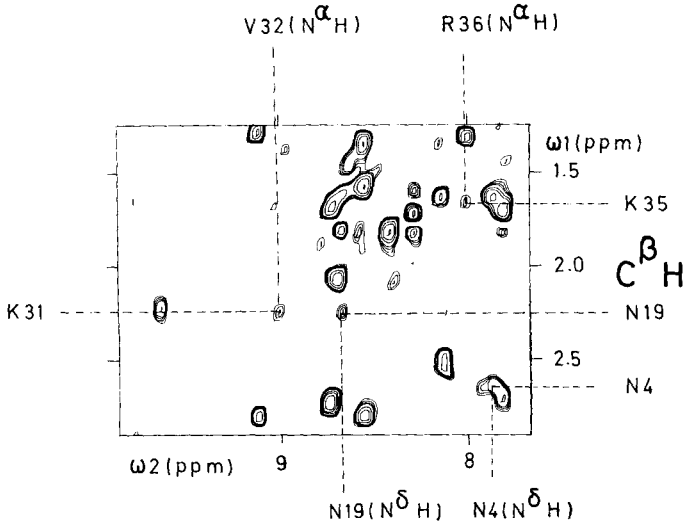

Fig. 10. *Contour plot of the spectral region (ω_1 = 1.2–2.8 ppm, ω_2 = 7.8–9.8 ppm) of the 500-MHz ^1H NOESY spectrum in Fig. 3.* The spectrum was recorded from a solution of toxin $V^{11}2$ in H_2O at pH 3.6 and 45 °C with a mixing time of 100 ms. The cross peaks which manifest the d_3 connectivities from residue 31 to 32 and from 35 to 36, and those used to assign the side chain amide protons of Asn-4 and Asn-19, are identified by dashed lines. The resonance assignments are indicated in the margins

residue can in principle be obtained from the J connectivities between NH, C$^{\alpha}$H and the side-chain protons obtained from COSY and SECSY (Fig. 4). Individual assignments were thus obtained for all the spin systems identified in Fig. 1 and 2. For residues with long side chains, such as Lys, Arg, Met and Pro, unambiguous identification of the C$^{\alpha}$H-C$^{\beta}$H$_2$ cross peaks in the SECSY spectrum was in some cases difficult. In these instances the assignments of the C-β protons were based on observation of d_3 connectivities and/or on NOEs between the amide proton and the C-β protons of the same residue. Thus, in toxin $V^{11}2$ the C-β protons of Lys-16, Lys-31, Lys-44 and Lys-50 were assigned via d_3 connectivities. For Met-26, Arg-27 and Met-52, NOEs between C$^{\beta}$H$_2$ and their own NH protons were observed. In the case of Met-24 both a d_3 connectivity to one C-β proton and an NOE from its own NH to the other C-β proton were used to assign the two C-β protons. Similarly, for Lys-18 and Pro-33 the SECSY spectrum yielded only one C-β proton position and the second C-β proton was found via a d_3 connectivity.

Since after the sequential assignments it was known for each of the C$^{\alpha}$H-C$^{\beta}$H$_n$ fragments to which type of amino acid residue it belonged, some of the more complex side chains could now be completely assigned. This is documented in Fig. 12 for Leu-6, Ile-7, Leu-20, Leu-48 and Ile-49. In addition to the information from the SECSY spectrum, data used for these assignments included that the δ-methyl triplets of the isoleucines were

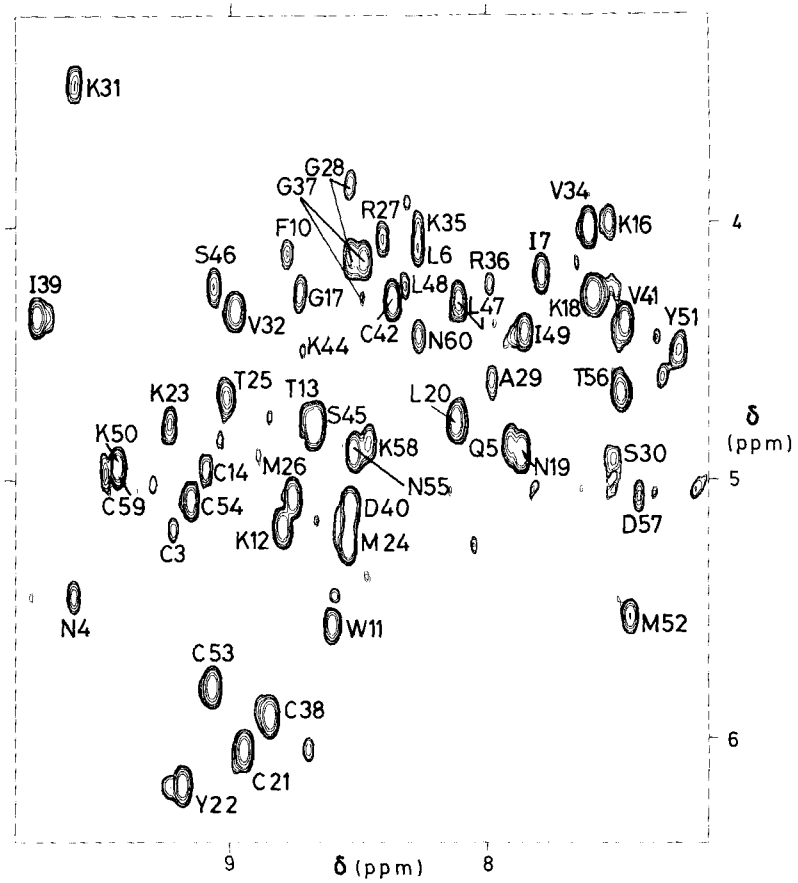

Fig. 11. *Spectral region (ω_1 = 3.2–6.4 ppm, ω_2 = 7.2–9.8 ppm) of a 500-MHz ^1H COSY spectrum recorded in a 0.01 M solution of toxin $V^{11}2$ in H_2O, pH 3.6, 45 °C.* The spectrum was recorded in about 39 h. The letters and numbers indicate the assignments for the C$^{\alpha}$H – NH J cross peaks in the protein. There is one peak for each residue except Leu-1 and Lys-2, and of course the prolines. For Gly-28 and Gly-37 there are two cross peaks, whereas for Gly-17 only one peak is seen

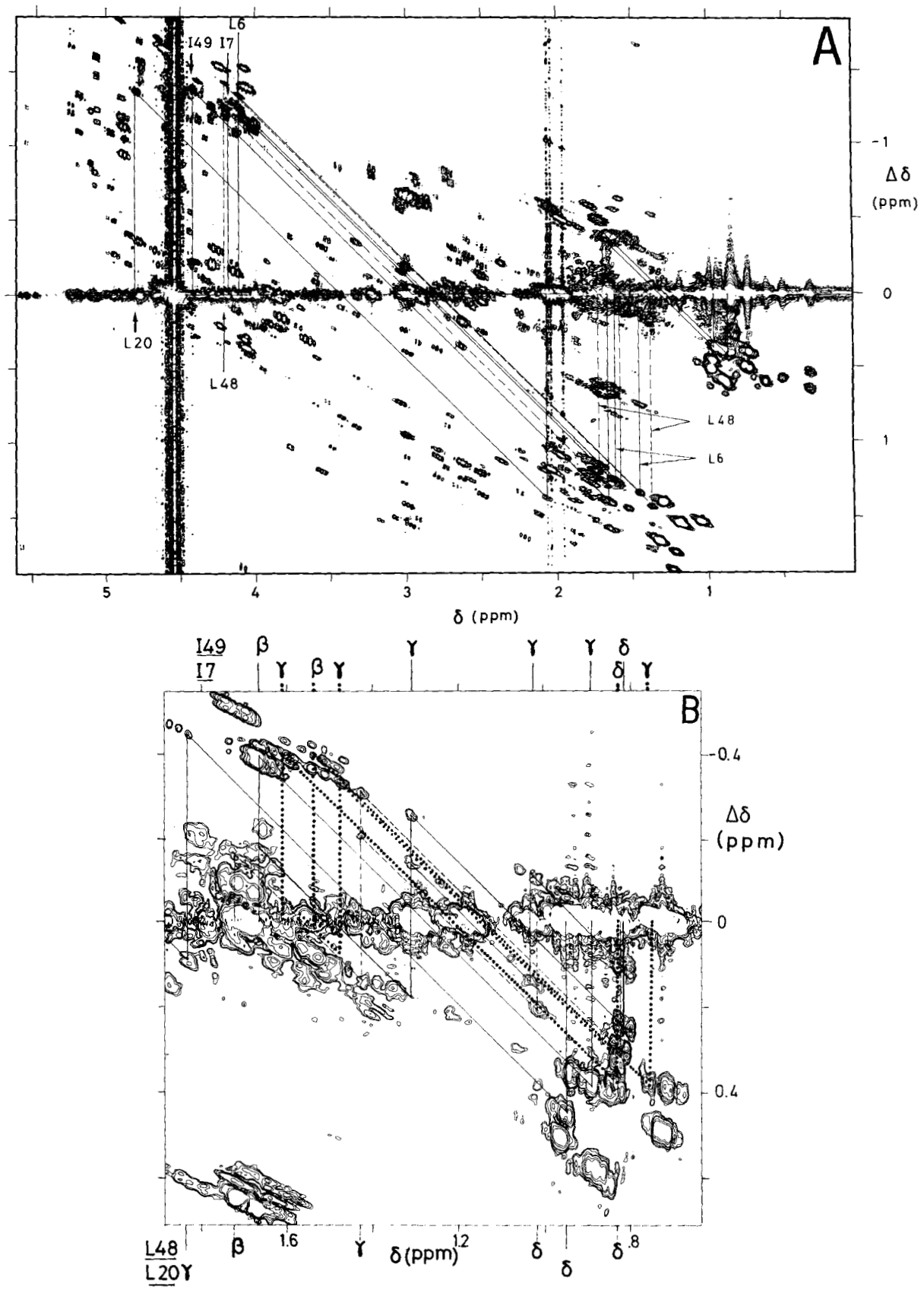

Fig. 12. *Contour plots of selected spectral regions of the 500-MHz ^1H SECSY spectrum of toxin $V^{11}2$ in Fig. 1 with the connectivities for the spin systems of Leu-6 (– – – –), Ile-7 (— —), Leu-20 (— — —), Leu-48 (· · ·), and Ile-49 (· — —).* For Leu-6 (– – – –) all the observed connectivities are shown in A; those between $C^{\beta}H$ and $C^{\beta'}H$, and between $C^{\beta}H$ and $C^{\gamma}H$, could not be resolved. For Ile-7 and Ile-49 (– · – · –) the $C^{\alpha}H-C^{\beta}H$ connectivity is shown in A and the connectivities for the peripheral segments in B. For Leu-20 only one $C^{\alpha}H-C^{\beta}H$ cross peak was found (A), and to this a fragment $C^{\gamma}H-C^{\delta}H_3$ could be connected (B). It could not be decided for Leu-20 whether the two β-methylene protons and/or the two δ-methyls are accidentally degenerate or whether part of the spin system was not observed. For Leu-48 all the hydrogen atoms could be assigned (A and B)

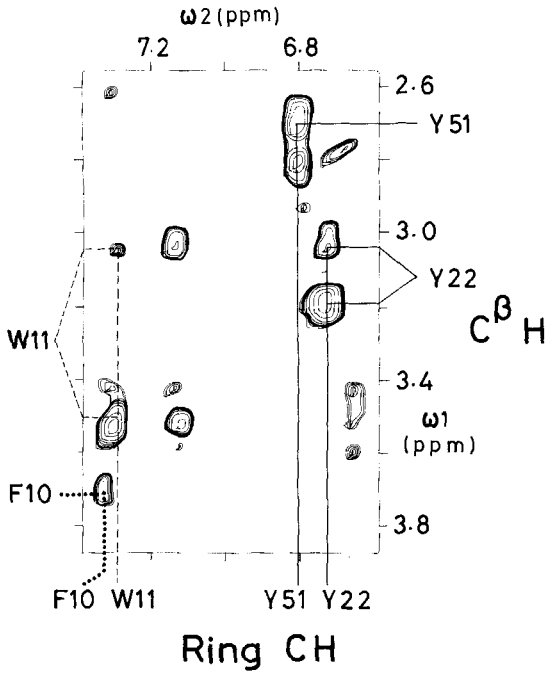

Fig. 13. *Spectral region (ω_1 = 2.6 – 3.8 ppm, ω_2 = 6.6 – 7.3 ppm) of a 500-MHz ^1H NOESY spectrum recorded in a 0.01 M ^2H_2O solution of toxin $V^{II}2$, p^{2}H 3.6, 45 °C.* For this solution, the protein was dissolved in ^2H_2O, heated to 50 °C for 2 h, lyophilised and then redissolved in ^2H_2O. This procedure was repeated to ensure complete exchange of all labile protons prior to the NMR experiment. The spectrum was recorded in about 40 h. The mixing time was 100 ms. NOE cross peaks from the aromatic ring protons to the corresponding C-β protons are shown by vertical lines at the chemical shift positions of the ring protons for Tyr-22 (——), Tyr-51 (— — —), Trp-11 (– · – ·) and Phe-10 (· · · · · ·). The C-β proton chemical shifts are indicated in the left and right margins of the figure

observed in a 2D *J*-resolved spectrum [29] and that an NOE was observed between the amide proton and C$^\gamma$H of Leu-6.

For Asn-4 and Asn-19, the δ-amide protons were assigned from the NOESY connectivities with the sequentially assigned C-β protons (Fig. 10) [32]. Finally, the previously identified [8] aromatic spin systems of Phe-10, Trp-11, Tyr-22 and Tyr-51 could be connected to the respective C$^\beta$H$_2$ by NOESY connectivities [32] (Fig. 13). The individual assignments for the two tyrosines, which had been proposed from comparison with homologous toxins [8], could thus be confirmed and the C-2,6 and C-3,5 protons for Phe and Tyr were unambiguously distinguished (Table 1).

DISCUSSION

The experiments in this paper represent an extension of earlier work where some or all ^{1}H NMR lines of 10 amino acid residues (these are identified in Table 1) were individually assigned by using one-dimensional and two-dimensional NMR in ^2H_2O solutions of toxin $V^{II}2$ [8]. These earlier assignments, some of which were based on comparison of homologous proteins, were now confirmed and based entirely on the method of sequential assignments; further new assignments were obtained for nearly all other residues of the polypeptide chain. The results are in most aspects comparable with those obtained with the same methods for other proteins of similar size [33, 49 – 51]. Except for the two N-terminal residues and two prolines, all the backbone hydrogen atoms were assigned. The side-chain assignments are complete, with the exception of the long side chains of Gln, Pro, Met, Lys and Arg, which have not usually been assigned in the other proteins [29, 33, 49 – 51], and Leu-1 and Leu-47. Also it may be added that in toxin $V^{II}2$ there are not less than 19 methyl doublets of Val, Leu and Ile crowded in a narrow spectral region (Fig. 1 and 12 and Table 1) which made unique assignments quite difficult in some cases.

With the resonance assignments in Fig. 5 and Table 1 all the strong cross peaks in the 'NMR fingerprint' [33] of toxin $V^{II}2$ (Fig. 11) were assigned and no peak was assigned more than once, which is one of the obvious checks on the sequential assignment procedure. However, Fig. 11 contains about 20 weaker peaks, which are all located near to assigned peaks. From the chemical shifts it can be excluded, in most cases, that these extra peaks could arise from spin-spin couplings with the labile protons in the side chains of Lys and Arg [52]. This leaves two alternative explanations. Firstly, experience with other proteins [51, 33] indicates that the extra peaks might correspond to small concentrations of chemically modified toxin $V^{II}2$, which could have been formed while the protein solution was kept at 45 °C during the NMR measurements, for example by deamidation of Asn and Gln side chains. Secondly, the extra peaks might manifest conformational heterogeneity. The occurrence of multiple conformations and sluggish conformational transitions under non-denaturing conditions has been observed for a variety of snake cardiotoxins in aqueous solution (unpublished data) and toxin $V^{II}2$ was actually selected for a more detailed study because the preliminary experiments provided no evidence for conformational heterogeneity [8]. We expect that the origin of the weak extra peaks will be further clarified by investigations of the spatial structure of toxin $V^{II}2$, which will include studies at various temperatures between 5° and 45 °C.

In the first paper on NMR of toxin $V^{II}2$ a small fragment of a triple-stranded β-sheet was identified, which includes residues 20 – 23 in the central strand and residues 36 – 39 and 53 – 54 in the peripheral strands. (This numbering system corresponds to that in Fig. 5 and is different from that used in [8].) The sequential connectivity patterns in Fig. 5, combined with observations on slowly exchanging amide protons, support this earlier structural interpretation and, further, provide evidence that the β-structure extends beyond the above-mentioned peptide segments. Since d_1 connectivities indicate an extended polypeptide structure, such as the individual strands in β-sheets, and continuous d_2 connectivities over several consecutive residues are indicative of an α-helical structure [32, 33, 46 – 48], Fig. 5 clearly indicates the presence of β-structure and lacks clear indications of α-helical secondary structure. Preliminary assignments of slowly exchanging amide protons were obtained by matching the chemical shifts of COSY cross peaks in a ^2H_2O spectrum of toxin $V^{II}2$ recorded at 25 °C with those of the assigned peaks in Fig. 11. Slow exchange is indicated for residues 11 – 13, 20 – 25, 34, 37, 39, 45, 51, 54 and 56. The sequential connectivities and the amide proton exchange data thus appear to be compatible with a β-sheet structure involving residues 20 – 25 as a non-peripheral strand, and the segments 33 – 39 and 51 – 56 as peripheral strands. These conclusions on the spatial structure are preliminary and further work is needed to check these statements and to use the resonance assignments described here as a basis for more extensive investigations of the three-dimensional structure of toxin $V^{II}2$.

We are grateful to Prof. M. Lazdunski (University of Nice) for providing us with the cardiotoxin $V^{II}2$ used fo the present study. Financial support by the *Schweizerischer Nationalfonds* (project 3.528.79) is grate-

fully acknowledged. We would like to thank Mrs E. Huber for the careful preparation of the manuscript.

REFERENCES

1. Low, B. W. (1979) in *Snake Venoms* (Lee, C.-Y., ed.) pp. 213–257, Springer-Verlag, Berlin.
2. Tu, A. T. (1977) *Venoms: Chemistry and Molecular Biology*, John Wiley & Sons, New York, London, Sydney, Toronto.
3. Rang, H. P. (1975) *Q. Rev. Biophys. 7*, 283–399.
4. Karlsson, E. (1979) in *Snake Venoms* (Lee, C.-Y., ed.) pp. 159–212, Springer-Verlag, Berlin.
5. Vincent, J. P., Balerna, M. & Lazdunski, M. (1978) *FEBS Lett. 85*, 103–108.
6. Dufourcq, J. & Faucon, J.-F. (1978) *Biochemistry, 17*, 1170–1176.
7. Vincent, J. P., Schweitz, W., Chicheportiche, R., Fosset, M., Balerna, M., Lenoir, M. C. & Lazdunski, M. (1976) *Biochemistry, 15*, 3171–3175.
8. Steinmetz, W. E., Moonen, C., Anil Kumar, Lazdunski, M., Visser, L., Carlsson, F. H. H. & Wüthrich, K. (1980) *Eur. J. Biochem. 120*, 467–475.
9. Arseniev, A. S., Balashova, T. A., Utkin, Y. N., Tsetlin, V. I., Bystrov, V. F., Ivanow, V. T. & Ovchinnikov, Y. A. (1976) *Eur. J. Biochem. 71*, 595–606.
10. Lauterwein, J., Wüthrich, K., Schweitz, H., Vincent, J. P. & Lazdunski, M. (1977) *Biochem. Biophys. Res. Commun. 76*, 1071–1078.
11. Inagaki, F., Miyazawa, T., Hori, H. & Tamiya, N. (1978) *Eur. J. Biochem. 89*, 433–442.
12. Lauterwein, J., Lazdunski, M. & Wüthrich, K. (1978) *Eur. J. Biochem. 92*, 361–371.
13. Bystrov, V. F., Arseniev, A. S. & Gavichov, Y. D. (1978) *J. Magn. Reson. 30*, 151–184.
14. Tsetlin, V. I., Arseniev, A. S., Utkin, Y. N., Gurevich, A. Z., Senyavina, L. B., Bystrov, V. F., Ivanov, V. T. & Ovchinnikov, Y. A. (1979) *Eur. J. Biochem. 94*, 337–346.
15. Fung, C. H., Chang, C. C. & Gupta, R. K. (1979) *Biochemistry, 18*, 457–460.
16. Endo, T., Inagaki, F., Hayashi, K. & Miyazawa, T. (1979) *Eur. J. Biochem. 102*, 417–430.
17. Inagaki, F., Tamiya, N. & Miyazawa, T. (1980) *Eur. J. Biochem. 109*, 129–138.
18. Arseniev, A. S., Pashkov, V. S., Pluzhnikov, K. A., Rochat, H. & Bystrov, V. F. (1981) *Eur. J. Biochem. 118*, 453–462.
19. Inagaki, F., Miyazawa, T. & Williams, R. J. P. (1981) *Biosci. Rep. 1*, 743–755.
20. Endo, T., Inagaki, F., Hayashi, K. & Miyazawa, T. (1981) *Eur. J. Biochem. 120*, 117–124.
21. Inagaki, F., Clayden, N. J., Tamiya, N. & Williams, R. J. P. (1981) *Eur. J. Biochem. 120*, 313–322.
22. Inagaki, F., Boyd, J., Campbell, I. D., Clayden, I. J., Hall, W. E., Tamiya, N. & Williams, R. J. P. (1982) *Eur. J. Biochem. 121*, 609–616.
23. Endo, T., Inagaki, F., Hayashi, K. & Miyazawa, T. (1982) *Eur. J. Biochem. 122*, 541–547.
24. Inagaki, F., Clayden, N. J., Tamiya, N. & Williams, R. J. P. (1982) *Eur. J. Biochem. 123*, 99–104.
25. Kimball, M. R., Sato, A., Richardson, J., Rosen, L. S. & Low, B. W. (1979) *Biochem. Biophys. Res. Commun. 88*, 950–959.
26. Low, B. W., Preston, W. S., Sato, A., Rosen, L. S., Searl, J. E. & Rudko, A. D. (1976) *Proc. Natl Acad. Sci. USA, 73*, 2991–2994.
27. Tsernoglou, D. & Petsko, G. A. (1977) *Proc. Natl Acad. Sci. USA, 74*, 971–974.
28. Tsernoglou, D. & Petsko, G. A. (1976) *FEBS Lett. 68*, 1–4.
29. Nagayama, K. & Wüthrich, K. (1981) *Eur. J. Biochem. 114*, 365–374.
30. Wagner, G., Anil Kumar & Wüthrich, K. (1981) *Eur. J. Biochem. 114*, 375–384.
31. Wüthrich, K., Wider, G., Wagner, G. & Braun, W. (1982) *J. Mol. Biol. 155*, 311–319.
32. Billeter, M., Braun, W. & Wüthrich, K. (1982) *J. Mol. Biol. 155*, 321–346.
33. Wagner, G. & Wüthrich, K. (1982) *J. Mol. Biol. 155*, 347–366.
34. Wider, G., Lee, K. H. & Wüthrich, K. (1982) *J. Mol. Biol. 155*, 367–388.
35. Chicheportiche, R., Vincent, J. P., Kopeyan, C., Schweitz, H. & Lazdunski, M. (1975) *Biochemistry, 14*, 2081–2091.
36. Aue, W. P., Bartholdi, E. & Ernst, R. R. (1976) *J. Chem. Phys. 64*, 2229–2246.
37. Nagayama, K., Anil Kumar, Wüthrich, K. & Ernst, R. R. (1980) *J. Magn. Reson. 40*, 321–334.
38. Bax, A. & Freeman, R. (1981) *J. Magn. Reson. 44*, 542–561.
39. Nagayama, K., Wüthrich, K. & Ernst, R. R. (1979) *Biochem. Biophys. Res. Commun. 90*, 305–311.
40. Jeener, J., Meier, B. H., Bachmann, P. & Ernst, R. R. (1979) *J. Chem. Phys. 71*, 4546–4553.
41. Anil Kumar, Ernst, R. R. & Wüthrich, K. (1980) *Biochem. Biophys. Res. Commun. 95*, 1–6.
42. Macura, S., Huang, Y., Suter, D. & Ernst, R. R. (1981) *J. Magn. Reson. 43*, 259–281.
43. Anil Kumar, Wagner, G., Ernst, R. R. & Wüthrich, K. (1980) *Biochem. Biophys. Res. Commun. 96*, 1156–1163.
44. Wider, G., Hosur, R. V. & Wüthrich, K. (1983) *J. Magn. Reson*, in the press.
45. Baumann, R., Wider, G., Ernst, R. R. & Wüthrich, K. (1981) *J. Magn. Reson. 44*, 402–406.
46. Dubs, A., Wagner, G. & Wüthrich, K. (1979) *Biochim. Biophys. Acta, 577*, 177–194.
47. Leach, S. J., Némethy, G. & Scheraga, H. A. (1977) *Biochem. Biophys. Res. Commun. 75*, 207–215.
48. Kuo, M. & Gibbons, W. A. (1979) in *Peptides: Structure and Biological Function, Proc. of the Sixth American Peptide Symp.* (Gross, E. & Meienhofer, J., eds) pp. 229–232, Pierce Chem. Co., Rockford.
49. Arseniev, A. S., Wider, G., Joubert, F. J. & Wüthrich, K. (1982) *J. Mol. Biol. 159*, 323–351.
50. Keller, R. M., Baumann, R., Hunziker-Kwik, E. H., Joubert, F. J. & Wüthrich, K. (1983) *J. Mol. Biol.* in the press.
51. Štrop, P., Wider, G. & Wüthrich, K. (1983) *J. Mol. Biol.* in the press.
52. Bundi, A. & Wüthrich, K. (1979) *Biopolymers, 18*, 285–298.

R. V. Hosur, G. Wider, and K. Wüthrich, Institut für Molekularbiologie und Biophysik
der Eidgenössischen Technischen Hochschule Zürich, Zürich-Hönggerberg, CH-8093 Zürich, Switzerland